

Imaging Diagnostics of Debris from Double Pulse Laser-Produced Tin Plasma for EUV Light Source

Tomoya Akiyama¹, Kota Okazaki², Daisuke Nakamura¹, Akihiko Takahashi², Tatsuo Okada¹

¹*Graduate School of Information Science and Electrical Engineering, Kyushu University,*

744 Motoooka Nishi-ku, Fukuoka 819-0395 Japan

²*Graduate School of Medical Sciences, Kyushu University,*

3-1-1 Maidashi, Higashi-ku, Fukuoka 812-8582 Japan

(Received: 26 August 2008 / Accepted: 2 February 2009)

The dynamics of debris from laser produced Tin (Sn) plasma was investigated for EUV light source. The kinetic behaviors of the Sn atoms and of the dense particles from Sn droplet target irradiated by double pulses from the Nd:YAG laser and the CO₂ laser were also investigated by the laser-induced fluorescence imaging method and a high-speed imaging, respectively. After the pre-pulse irradiation of the Nd:YAG laser, the Sn atoms were ejected in all direction from the target with a speed of as fast as 20 km/s and the dense particle cloud expanded by a reaction force due to the plasma expansion with a speed of approximately 500 m/s. The expanding target was subsequently irradiated by the main-pulse of CO₂ laser and the dense cloud was almost disappeared by main-pulse irradiation.

Keywords: EUV , droplet , debris , LPP , double pulse , LIF imaging , shadowgraph , neutral atoms

1. Introduction

Extreme ultraviolet (EUV) lithography is one of the most promising next generation lithography tools used in the semiconductor industry to produce electronic nodes with a critical size of 32 nm or less. However, EUV lithograph is facing several challenges to satisfy requirements. One of those is to develop a powerful, clean, and long lifetime EUV light source. In a practical EUV lithography system, it is said that an average EUV power of 180 W in 2 %-bandwidth around 13.5 nm at the intermediate focus is required [1]. EUV light sources have been under development based on the laser-produced plasma (LPP) or the discharge-produced plasma (DPP) [2]. In the case of LPP, the tin (Sn) plasmas produced by CO₂ lasers at a wavelength of 10.6 μm have been considered to be the most promising EUV light source [3, 4]. For Sn target, a conversion efficiency of about 3%, which is higher than any other material, has been obtained. However, the generation of debris that damages collector optics and limits the lifetime of the optical system is more critical problem in the case of Sn target. Therefore, a mitigation of the debris is most importance for the development of a practical EUV lithography system. Several methods are developed to mitigate the debris. But it is difficult to mitigate the neutral particle debris because they can not be controlled by electromagnetic field. In the previous study, it was found that the neutral atoms are originated from the low-intensity part of the laser spot and the deep layer from the target surface [5] and large size debris must be also generated from the same parts. So, the general approach for debris mitigation is the use of a minimum amount of Sn that can provide a sufficient

EUV power. This type of the Sn target is called as a mass-limited or a minimum-mass target [6-8].

One of the general mass-limited targets is Sn droplets with a size of several tens of micrometers in diameter. In the use of the droplet target and CO₂ laser, however, it is required that Sn micro-droplets have to be expanded by 10-20 times before CO₂ laser irradiation, in order to improve the coupling efficiency between long-wavelength CO₂ laser and micro-droplets. For the purpose, the pre-irradiation of a Q-switched Nd:YAG laser at a wavelength of 1064 nm prior to the main CO₂ laser irradiation is one of the promising schemes. This scheme is called the double pulse irradiation (DPI) technique [8]. In the DPI scheme, the ablation dynamics of laser-irradiated Sn droplet are very important for attempting to optimize DPI operation and mitigate the debris.

In this report, we describe the ablation dynamics of a Sn droplet irradiated by double laser pulses from a Nd:YAG laser and a CO₂ laser. The spatial distribution of the Sn atoms from the Sn plasma was visualized by the laser-induced fluorescence (LIF) imaging method. While, the temporal behavior of dense particles from the droplet were visualized in synchronized with LIF imaging using a high-speed framing camera in single ablation event.

2. Experimental Setup

Fig.1 shows the experimental setup for investigation of debris in DPI scheme. It consists of a Q-switched Nd:YAG laser as a pre-pulse laser, and a CO₂ laser as a main-pulse laser, a vacuum chamber with a target holder, and time-resolved two-dimensional LIF imaging and

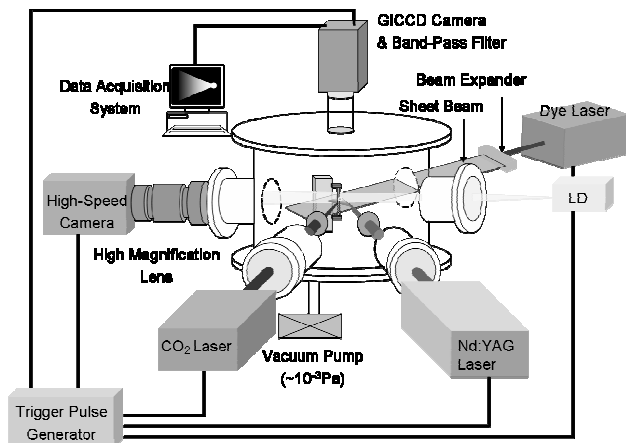


Fig. 1 Experimental Setup

shadowgraph imaging systems. An output energy of the Nd:YAG laser (Spectra Physics, Quanta-Ray Pro) was 1 J with a Q-switched pulse of 8 ns in FWHM at a wavelength of 1.064 μm and CO₂ laser (Lambda Physik EMG201MSC) with a gain switched pulse of 50 ns in FWHM followed by a low-intensity tail lasting for about 1 μs . CO₂ laser and Nd:YAG laser have a spot diameter of approximately 500 μm and 40 μm , respectively. The both beams were in the x-y plane and the angle between the two beams was 45 degrees. The target was a Sn droplet which was made with a help of a pulsed-laser irradiation, and the droplet size was 30 μm in a diameter. We attached the droplet on a polyamide fiber of 10 μm diameter as the target for laser irradiation. The Nd:YAG laser beam was aligned at a normal incidence on the target surface. The chamber was evacuated at a pressure of 10^{-3} Pa by a vacuum pump.

In the LIF imaging for Sn atoms, a planar sheet laser beam from a tunable dye laser (Spectra-Physics Sirah) at a wavelength of 286.327 nm was passed in the plane of the target. More detailed information about LIF imaging has been described in the previous report [5]. The shadowgraph images were captured by a high-speed framing camera (Hadland Photonics Ltd. Imacon468) with a back-light from a cw laser diode (Sacher Lasertechnik littrow TEC-120) at a wavelength of 848 nm. The high-speed framing camera could take 5 frames with each different delay time in single event. The camera was triggered by the pulse generator in synchronizing with the LIF system and the gate width was set to 100ns.

3. Behavior of Neutral Atoms Irradiated by a Pre-pulse

The behavior of neutral atoms irradiated by a pre-pulse was investigated with LIF imaging. Fig. 2 shows the temporal resolved image in the spatial distribution of Sn atoms. The pre-pulse laser was irradiated to the target from left side of the image and the target located at the center of the image before the irradiation. It was observed

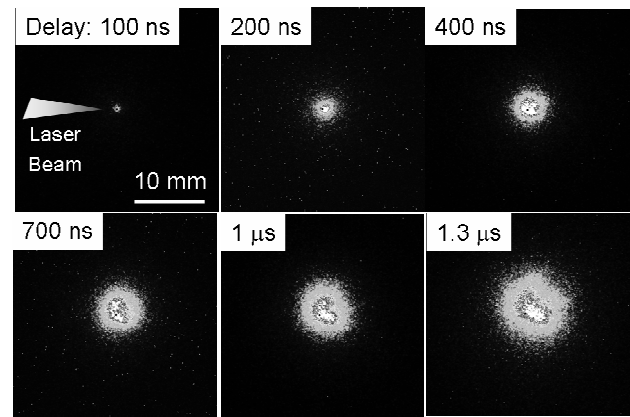


Fig. 2 The Time-resolved LIF imaging

that the Sn atoms were emitted in all direction from the target. The kinetic speed of the Sn atoms at the expanding front was estimated to be approximately 20 km/s from the image of 400 ns delay. The directional distributions of the ejected species are generally governed by the curvature of the target surface. In the case of the flat plate target, Sn atoms are ejected along the target surface normal due to steep pressure gradient, and results in the forward-peaked distribution. In the case of the micro-droplet target, on the other hand, it is considered that since the size of the laser-produced plasma was larger than the curvature of the target surface, the Sn atoms were ejected to the opposite side of the target due to the reaction force due to the plasma expansion.

4. Behavior of Droplet Target Irradiated by a Pre-pulse

4-1 Behavior of the dense particles

The behavior of droplet target irradiated by the pre-pulse was investigated with shadowgraph imaging. It is shown in Fig 3. The Nd:YAG laser at the intensity of 4.8×10^{11} W/cm² was irradiated from left side of the shadowgraph image. The observation direction was 135 degrees from the pre-pulse incidence. In the image of 0 ns, the fiber that sustained the droplet was cut instantaneously by the laser-produced plasma. After 200 ns, the dense particle cloud, that may consisted of small molten Sn particles or clusters, expanded by a reaction force from due to the plasma expansion. In order to measure in detail the behavior of the expanding dense cloud, the shadowgraph was observed at a normal angle from the pre-pulse laser incident direction. As a result, the dense cloud moved to the opposite side of the laser incident direction with expansion and the drift velocity was estimated to be approximately 500 m/s. After delay times of 600 ns to 800 ns, the dense cloud at early delay was gradually vanished by expansion and vaporization. Several dozen particulates were collected on the surface of the witness plate as shown in Fig.4. The volume of the

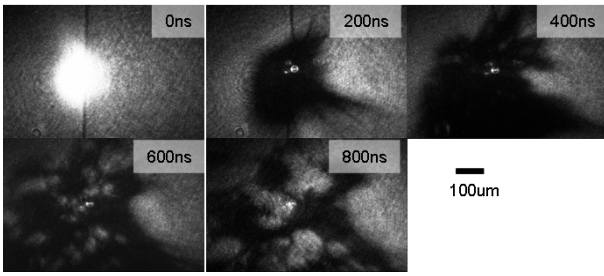


Fig.3 The shadowgraphs of the irradiated target debris at different delay times after pre-pulse irradiation

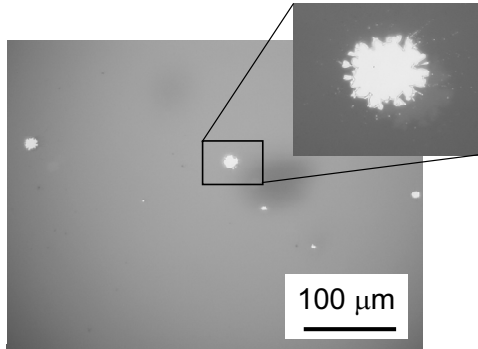


Fig.4 The optical microscope image of dozen particulates on the surface of the witness plate.

particulates was measured using an atomic force microscope and converted to the diameter of the sphere that has the same volume of particulates. In result, the estimated diameter was in the range of about 1-6 μm . Thus, it was confirmed that neutral atoms and small liquid debris were generated from the droplet target irradiated by single pulse of Nd:YAG laser. It was also checked that the dense cloud and the particulates in Fig. 3 were not from the fiber, but from the Sn droplet, by comparing the images with and without the Sn droplet on the fiber.

4-2 Influence of the pre-pulse intensity

Next, we investigated an influence of the pre-pulse intensity on the ablation dynamics. Fig.5 shows the shadowgraphs of the irradiated target at different intensities of pre-pulse. The expanding speed of the dense cloud increases with increasing the intensity of the pre-pulse. At the intensity of $1.1 \times 10^{12} \text{ W/cm}^2$, the dense cloud was expanded more than the observation area at 200 ns after laser irradiation. And the cloud seems to disappear from its central part because of the plasma expansion. At the intensity of $3.4 \times 10^9 \text{ W/cm}^2$, on the other hand, the cloud was expanded to about $100 \mu\text{m}$ after 800 ns delay. The target was hardly expanded at the intensity less than 10^8 W/cm^2 .

5. Behavior of Droplet Target Irradiated by Double Pulse

The behavior of droplet target irradiated by pre-pulse was mentioned above. Based on these results, the ablation dynamics of the target by double pulses of Nd:YAG and CO_2 laser was investigated. The pre-pulse of Nd:YAG laser irradiated the droplet target with a fluence of $2.0 \times 10^{11} \text{ W/cm}^2$, which was derived from the results of Fig.5 to expand the target within $1 \mu\text{s}$ sufficiently. The main-pulse of CO_2 laser irradiated the dense cloud after pre-pulse irradiation with a fluence of $1.8 \times 10^9 \text{ W/cm}^2$. A delay time of the main-pulse was proposed to be 800 ns, that the dense cloud expanded by the pre-pulse had almost the same size as that of the CO_2 laser beam. Fig.7 shows the Sn droplet target irradiated by the double pulses at different delay times after pre-pulse irradiation. At a delay of 800 ns, the plasma radiation produced by CO_2 laser irradiation was observed. At 600 ns, the dense

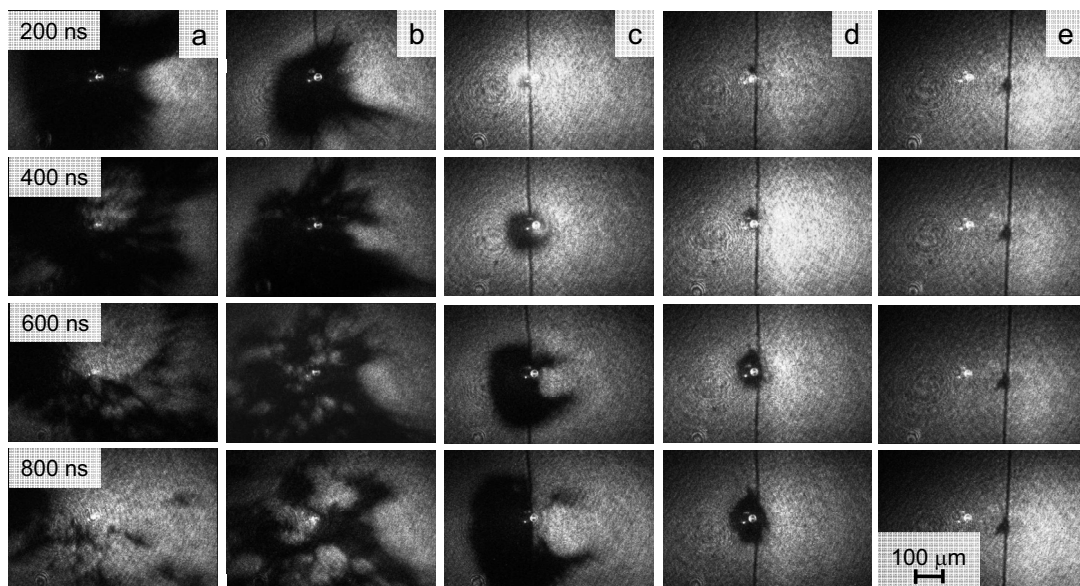


Fig.5 The shadowgraphs of the irradiated target debris at different delay times after pre-pulse irradiation at the laser intensities of (a) $1.1 \times 10^{12} \text{ W/cm}^2$, (b) $4.8 \times 10^{11} \text{ W/cm}^2$, (c) $1.6 \times 10^{11} \text{ W/cm}^2$, (d) $3.4 \times 10^9 \text{ W/cm}^2$, and (e) $5.4 \times 10^8 \text{ W/cm}^2$.

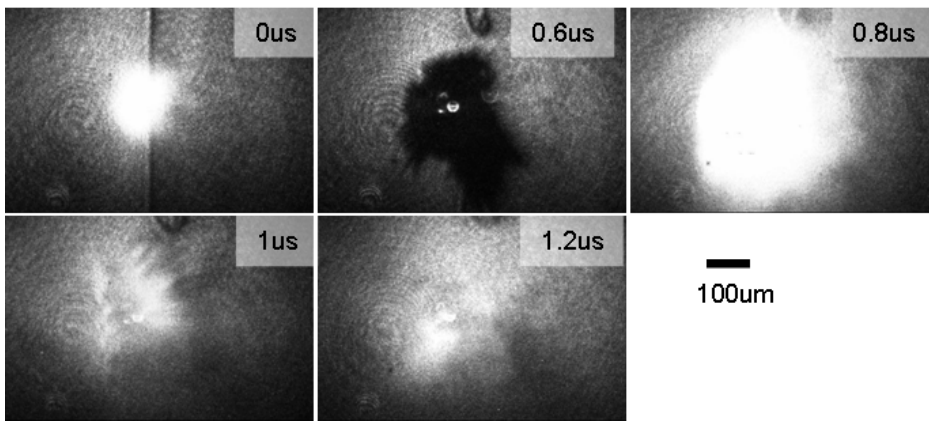


Fig. 6 The shadowgraphs of the target irradiated by the double pulses of Nd:YAG laser and CO₂ laser at a delay of 800ns.

cloud was observed as in Fig. 5(C), but after CO₂ laser irradiation the dense cloud disappeared. Thus it was found that the DPI scheme was also useful the mitigation of the particulates. Regarding the mitigation of Sn atoms, on the other hand, it should be noticed that the fast Sn atoms were already expanded around about 5mm in diameter even at the delay of 400 ns, as shown in Fig. 3. Therefore, Sn atoms are inevitably generated, as long as the Q-switched Nd:YAG laser is used as the pre-pulse laser in order to expand the target within 1 μ s in the DPI scheme. In addition, the expansion speed limits the repetition rate in DPI scheme. The expansion condition of the dense cloud strongly depends on the pre-pulse energy that hit the target, as shown in Fig. 5. At low intensity, more time is required before the dense cloud expands up to the size of the CO₂ laser beam.

6. Summary

The ablation dynamics of the Sn micro-droplet in the DPI scheme for EUV lithography source was investigated by the LIF imaging system and the shadowgraph framing system. In the present DPI, a Q-switched Nd:YAG laser and a CO₂ laser are used as a pre-pulse for the target expansion and a main-pulse for the plasma production, respectively. It was found that the fast Sn atoms are ejected in all directions with a speed of as fast as 20 km/s by pre-pulse irradiation and the dense Sn cloud expands with a speed of about 500 m/s. The expanding speed of the dense cloud increases with increasing the intensity of the pre-pulse. It takes about 800 ns for the micro Sn droplet to expand to the size of around 500 μ m in diameter with a fluence of 2.0×10^{11} W/cm² before the main-pulse irradiation. After CO₂ laser irradiation the dense cloud disappeared. On the other hand, however, Sn atoms are inevitably generated, as long as the Q-switched Nd:YAG laser is used as the pre-pulse laser in the DPI scheme, in order to expand the target to a comparable size as the main CO₂ laser beam within 1 μ s. Furthermore, the arraignment of the pre-pulse beam and the target is important for the distribution of the dense cloud in DPI scheme

7. Acknowledgments

A part of this work was performed under the contract subject "Leading Project for EUV lithography source development" and the auspices of MEXT (Ministry of Education, Culture, Science and Technology, Japan) and was supported by a Grant-in-Aid for Scientific Research No. 20760025 from Japan Society for the Promotion of Science.

References

- [1] U. Stamm: J. Phys. D 37, (2004) 3244.
- [2] V. M. Borisov, A. V. Eltsov, A. S. Ivanov, Y. B. Kiryukhin, O. B. Khristoforov, V. A. Mishchenko, A. V. Prokofiev, A. Y. Vinokhodov, V. A. Vodchits: J. Phys. D 37, (2004) 3254.
- [3] H. Tanaka, K. Akinaga, A. Takahashi, T. Okada: Jpn. J. Appl. Phys. 43, (2004) L585.
- [4] H. Tanaka, A. Matsumoto, K. Akinaga, A. Takahashi, T. Okada: Appl. Phys. Lett. 87, (2005) 041503.
- [5] H. Tanaka, Y. Hashimoto, K. Tamaru, A. Takahashi, T. Okada: Appl. Phys. Lett. 89, (2006) 181109.
- [6] S. Namba, S. Fujioka, H. Nishimura, Y. Yasuda, K. Nagai, N. Miyanaaga, Y. Izawa, K. Mima, K. Takiyama: Appl. Phys. Lett. 88, (2006) 171503.
- [7] M. Richardson, C. S. Koay, K. Takenoshita, C. Keyser: J. Vac. Sci. Technol. B 22, (2004) 785.
- [8] M. Shimomura, S. Fujioka, T. Ando, H. Sakaguchi, Y. Nakai, Y. Yasuda, H. Nishimura, K. Nagai, T. Norimatsu, K. Nishihara, N. Miyanaaga, Y. Izawa, K. Mima: Appl. Phys. Exp. 1, (2008) 056001